

Adaptively Clustering Neighbor Elements for Image Captioning

Zihua Wang^{1,2} Xu Yang¹ Haiyang Xu² Hanwang Zhang³ Qinghao Ye² Chenliang Li²
Weiwei Sun¹ Ming Yan² Songfang Huang² Fei Huang² Yu Zhang¹

¹ School of Computer Science & Engineering, Key Lab of Computer Network
& Information Integration (Ministry of Education), Southeast Univ., Nanjing, China

²DAMO Academy, Alibaba Group

³ School of Computer Science & Engineering, Nanyang Technological Univ., Singapore.

{zihua, 101013120, 213211492, zhang-yu}@seu.edu.cn, {shuofeng.xhy, yeqinghao.yph,
lcl193798, yml19608, songfang.hsf, f.huang}@alibaba-inc.com, hanwangzhang@ntu.edu.sg

Abstract

We propose a novel Transformer-based captioning model termed as **Ada-ClustFormer (ACF)** that can adaptively cluster vision patches into object regions and language words into phrases to implicitly learn object-phrase alignments for better captions. To achieve this, we design a novel self-attention layer that applies self-attention over the elements in a local cluster window instead of the whole sequence. The window size is softly decided by a clustering matrix that is calculated by the current input data and thus the clustering process is adaptive. By stacking these revised self-attention layers to construct ACF, the small clusters in the lower layers can be grouped into a bigger cluster, e.g., vision/language ACF clusters small objects/phrases into a bigger one. In this gradual clustering process, a parsing tree is also generated which embeds the hierarchical knowledge of the input sequence. As a result, by using ACF to build the vision encoder and language decoder, the hierarchical object-phrase alignments are embedded and then transferred from vision to language domains for more grounded captions. The experiment results demonstrate the effectiveness of ACF that we achieve a CIDEr of 138.3, which outperforms most SOTA captioning models and achieve comparable scores compared with some BERT-based models. The code will be available in the supplementary material.

1. Introduction

Image captioning [23] aims at generating a sentence to exhaustively describe multi-aspects of an image, which has achieved great progress since the proposal of attention-based encoder-decoder pipeline [48, 43]. Nowadays, both the vision encoder and the language decoder are built

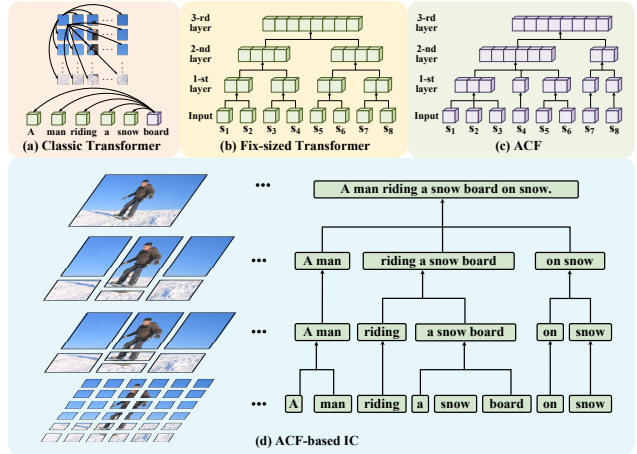


Figure 1. (a) The classic Transformer. (b) Transformer with fixed-size windows (size = 2); (c) ACF which adjusts the window size according to the input. (d) ACF-based IC. The left/right part shows how the vision/language ACFs cluster image grids/language words for transferring structural commonalities.

based on Transformer [41] where the encoder learns the visual context knowledge by applying self-attention over the whole vision tokens and the decoder will softly select the suitable vision knowledge based on the context knowledge of the partially generated caption to generate the next word [21, 14].

While intuitively, when we humans describe an image, we usually first construct suitable phrases to describe the recognized important image regions and then compose these phrases into an integral sentence. However, as shown in Figure 1 (a), the aforementioned Transformer-based captioning models can not achieve such region-phrase alignments since the self-attention is applied over all the input tokens. As the result, each vision token output from the encoder embeds the context knowledge of the whole image instead of the neighbor regions. Similarly, when the

decoder generates the next word, the context of all the partially generated words is used to select the suitable vision knowledge.

To learn region-phrase alignment, the encoder and decoder at least should learn the local contexts. Motivated by this, various Transformer variants [2, 25] are proposed to implement self-attention over a cluster of neighbor elements in a fixed-size small window to learn local contexts. Moreover, when stacking these cluster-constrained self-attention layers, the small cluster in the lower layer will be gradually merged into bigger ones for learning more global knowledge. As a result, the local-global knowledge can be learnt by these Transformer variants. For example, as shown in Figure 1(b), the 1-st layer clusters 2 neighboring elements like $\{s_1, s_2\}$ to carry Self-ATT for local contexts and the 2-nd layer merges $\{s_1, s_2\}$ and $\{s_3, s_4\}$ into a bigger one to learn more global context.

However, these global-local Transformers can not be directly used to build captioning models to learn region-phrase alignments due to two reasons. Firstly, most previous local-global Transformers only use **fixed-size windows** to group tokens, while vision and language data have **varying graininess**, *e.g.*, objects/phrases different numbers of grids/words at different positions, and such varying graininess cannot be learnt by these fixed-size window-based self-attentions. Secondly, to encourage an encoder-decoder to learn region-phrase alignments, the **similar inductive bias** should be applied to design both the encoder and decoder. However, most local-global Transformers [36, 49] are exclusively designed to deal with images that exploit lots of visual inductive bias like translation invariance, which cannot be used as the language decoder.

To solve these two limitations, we propose a novel global-local Transformer which applies a general visual-linguistic inductive bias to capture varying graininess of both vision and language data. Specifically, we enable the self-attention layer to **Adaptively Cluster** the neighbor elements for implementing self-attention and term this novel model as **Ada-ClustFormer (ACF)**. To achieve this, we insert a probabilistic clustering matrix C into the self-attention layer, where the probability C_{ij} softly determines whether the sub-sequence $\{s_i, \dots, s_j\}$ should be clustered or not. To calculate C_{ij} , we consider whether the next element s_j is similar to the mean-pooling of $\{s_i, \dots, s_{j-1}\}$. Thus we can adjust the cluster size based on each specific data sample. As shown in Figure 1(c), in each layer, the window size is not fixed but can be adjusted to each specific input sequence, *e.g.*, in the 1-st layer, $\{s_1, s_2, s_3\}$, $\{s_4\}$, $\{s_5, s_6\}$, $\{s_7\}$, $\{s_8\}$ are respectively clustered. Then ACF can be constructed by stacking these revised self-attention layers, while simply stacking can not guarantee the small clusters in the lower layers to be merged into bigger ones in the higher layers. To remedy this problem, we enforce

$C^{l-1} \leq C^l$, where l denotes the l -th layer, by using a convex combination technique. Then as Figure 1(c) shows, the higher layers merge small clusters into bigger ones for learning global contexts, *e.g.*, the 2-nd layer respectively merges $\{s_1, s_2, s_3, s_4, s_5, s_6\}$, $\{s_7, s_8\}$ into two clusters to carry Self-ATT.

To construct an IC model based on ACF, besides building 1-D ACF for the language decoder, we also extend it to the 2-D ACF as the vision encoder to merge 2-D image patches into bigger ones. Moreover, we design two strategies to reduce the cost of calculating the clustering matrix C for the 2-D case, which are: (1) using independence assumption to decompose the 2-D distribution into two 1-D calculation, *i.e.*, the horizontal and vertical dimension, (2) down-up sampling strategy. By using vision ACF as the encoder and language ACF as the decoder, the built captioning model exploits the same inductive bias to discover hidden structures to learn better region-phrase alignments. For example, as Figure 1(d) shows, the patches of the object “snow board” and the phrase “a snow board” are respectively adaptively clustered. To sum up, our contributions are:

- We propose a novel **Ada-ClustFormer** that can adaptively cluster the neighbor elements for carrying self-attention (Self-ATT) to learn global-local contexts.
- We design both 1-D and 2-D ACF for building a homogeneous captioning model to transfer more structural commonalities for better captions.
- We propose two strategies which are independence decomposition and down-up sampling to reduce the computation burdens of 2-D ACF.
- We carry out exhaustive experiments to validate the effectiveness of the ACF-based captioning model.

2. Related Work

Image Captioning (IC). IC aims to generate descriptions according to the given images. Typically, an encoder-decoder paradigm is used to convert visual inputs to sequence outputs. In the early stage, image features are extracted by CNN-based encoders, as the input of the RNN-based decoders [4, 38, 43, 17, 8, 26]. For example, Up-Down [4] employs a Faster R-CNN [37] to extract image region features and LSTM networks to generate sentences. K-adaptive [26] proposes a memory store to decide whether to focus on the CNN encoder or the LSTM decoder.

Nowadays, Transformer-based models have shown their might in Neural Language Process (NLP) and replace RNN-based decoders in IC [21, 14, 16]. Subsequently, more advanced Transformer-based decoders are proposed, *e.g.*, \mathcal{M}^2 Transformer [9] proposes a meshed-memory Transformer to interact with the low-level and high-level features; X-Linear Transformer [33] selectively capitalizes the visual information from image regions by bilinear pooling.

However, these models still use CNN-based feature extractors. More recently, witnessing the boom of Vision Transformers (ViT) [11, 25], researchers use ViT-based visual encoders for captioning. For instance, CPTR [24] introduces grid-based features that are extracted by ViT [11] instead of using the ROI-based features; DLCT [27] fuses the ROI-based features with the grid-based features to overcome the shortcoming of both features. Besides that, some models exploit the knowledge distilled from Vision-Language BERTs for better captions [19]. VinVL [55] and GRIT [31] combine the object detection model with IC. ClipCAP [30], LEMON [15], and mPLUG [20] introduce large-scale pretraining into IC. Noteworthy, the methods above employ the ViT [11] or Swin Transformer [25] as their backbone.

Among the previous IC models, Auto-Parsing Network (APN) [50] has a similar motivation as ours, which also inserts a clustering matrix into the Self-ATT layer. However, Ada-ClustFormer (ACF) calculates this matrix differently. APN only considers whether pairwise neighboring elements should be clustered or not, while we calculate this probability from a more global scope. Specifically, we consider whether the next element is similar to the previous clustered elements. More importantly, we extend our ACF into the 2-D case, which can adaptively cluster the visual patches into regions, while APN only treats a sequence of ROI features as the visual input and still applies a 1-D clustering matrix to address it. More comparisons will be given in the supplementary material.

Global-Local Transformer. To alleviate the fully connected graph prior in Transformer, researchers propose various global-local Transformers to learn sparse structures of the language [28, 6]. For example, Global-local [28] introduces a fixed-size of the global and local attention model in neural machine translation. Transformer-XL [10] learns context by a segment-level recurrence mechanism. Longformer [6] proposes global and local window attentions, which can provide inductive bias and long sequence representation, respectively. Hi-Transformer [46] learns sentence-level and document-level semantics through the hierarchical structure.

The global-local Transformer mechanism is also effective in vision area [7, 56, 27]. Pairwise and patchwise self-attention are proposed in image recognition [56]. Furthermore, GLiT [7] proposes to adaptively trade off the global and local information of the images. DLCT [27] explores the global and local information by the combination of grid-based features and ROI-based features.

However, these models are exclusively developed in a single domain (either NLP or CV), while our ACF provides a general approach in both the vision and language domains. Thus, using ACF to build the IC model encourages learning a unified structure space for transferring more structure

commonalities.

3. Ada-ClustFormer IC model

Compared with the classic Transformer, Ada-ClustFormer (ACF) inserts an adaptively clustering matrix C into each self-attention (Self-ATT) layer to adaptively control the scope of Self-ATT. The calculation of C is detailed in Section 3.1 where we first show the 1-D language case and then extend it to the 2-D vision case. By stacking these revised Self-ATT layers, ACF can be built for constructing the vision encoder and language decoder for captioning (cf. Section 3.2).

3.1. Ada-ClustFormer

Multi-Head Attention (MHA). ACF is built based on Transformer, whose most elemental building block is the Multi-Head Attention (MHA). Given the query $Q \in \mathbb{R}^{N_Q \times d}$, key $K \in \mathbb{R}^{N_K \times d}$, and value $V \in \mathbb{R}^{N_V \times d}$, MHA calculates the output $Z = \text{MHA}(Q, K, V)$ as:

$$\begin{aligned} \text{Input: } & Q, K, V \\ \text{ATT: } & A_l = \text{Softmax}\left(\frac{QW_l^Q(KW_l^K)^T}{\sqrt{d}}\right) \\ \text{Head: } & H_l = A_l V W_l^V, \\ \text{Multi-Head: } & H = [H_1, H_2, \dots, H_h] W^H, \\ \text{Output: } & Z = \text{LN}(H + Q), \end{aligned} \quad (1)$$

where $W_l^Q, W_l^K, W_l^V \in \mathbb{R}^{d \times d_h}$, $W_l^H \in \mathbb{R}^{d \times d}$ are all learnable parameters; h denotes the head number and $d_h = d/h$; A_l is the l -th attention matrix corresponding to the l -th head H_l ; $[\cdot]$ is the concatenation operation; and LN denotes to the Layer Normalization.

Given an input sequence $S = \{s_1, \dots, s_N\}$, if $Q = K = V = S$, Eq. (1) is also called self-attention (Self-ATT). Self-ATT captures the global contexts between any two elements s_i and s_j by calculating the pairwise attention weight in the “ATT” operation. From the perspective of structure learning [5], single-head Self-ATT constructs a fully-connected (FC) graph where the nodes are the elements of S and the pairwise edges are weighted by the pairwise attention weight. Correspondingly, a h -head Self-ATT constructs h FC graphs with different edge weights.

Adaptive Clustering Matrix C . To sparsify this FC-graph, researchers [11, 25] propose to carry Self-ATT in fixed-size windows, which is achieved by revising “Head” in Eq. (1):

$$\text{C-based Head: } H = \text{Softmax}(A \otimes C) V W^V, \quad (2)$$

where “ \otimes ” denotes the element-wise production; C is a $N \times N$ **binary** clustering matrix that only the elements in the window can attend to each other, i.e., if the window size is w , $C_{i,j} = 1$ if $|i - j| \leq w$ and $C_{i,j} = 0$ if $|i - j| > w$. However, language or vision data usually

have diverse graininess, *e.g.*, a phrase may contain different numbers of words or an object may cover diverse spatial regions, while the fixed-size windows can not capture the varying graininess.

To amend this, we revise the binary C to a **probabilistic** one where $C_{i,j}$ softly determines whether to cluster the embeddings from s_i to s_j for carrying Self-ATT. Then if $C_{i,j}$ is small, the pairwise attention in \mathcal{A} between s_i and s_j is weakened in Eq. (2), which means s_i and s_j are less likely to stay in the same cluster. To adaptively decide the window size according to each specific input for capturing the varying graininess, we use the input itself to calculate $C_{i,j}$:

$$C_{i,j} = P(s_i, \dots, s_j) = \prod_{k=i}^j P(s_k | s_i, \dots, s_{k-1}), \quad (3)$$

where the joint distribution is decomposed to the productions of conditional distributions $P(s_k | s_i, \dots, s_{k-1})$, which softly decides whether to merge a new element s_k into the sub-sequence $\{s_i, \dots, s_{k-1}\}$. In the implementation, $P(s_k | s_i, \dots, s_{k-1})$ is calculated as:

$$P(s_k | s_i, \dots, s_{k-1}) = \text{Sigmoid}(\text{FC}([s_k, s_{i:k-1}]])), \quad (4)$$

where $s_{i:k-1}$ is the mean pooling of the embeddings from s_i to s_{k-1} . Intuitively, Eq. (4) exploits the context of the whole sub-sequence $\{s_i, \dots, s_{k-1}\}$ to decide whether to merge a new element $\{s_k\}$ into this sub-sequence. Note that Eq. (3) and Eq. (4) only make sense when $i < k$. Since clustering the embeddings from s_i to s_k equals to clustering from s_k to s_i , we set $C_{i,k} = C_{k,i}$ if $i > k$ and since a single element s_i is itself a cluster, we set $C_{i,i} = 1$.

From Eq. (3), we can also find that:

$$\begin{aligned} C_{i,j} &= P(s_j | s_i, \dots, s_{j-1}) \times P(s_i, \dots, s_{j-1}) \\ &= P(s_j | s_i, \dots, s_{j-1}) \times C_{i,j-1}. \end{aligned} \quad (5)$$

Since $P(s_j | s_i, \dots, s_{j-1}) \leq 1$, we have $C_{i,j} \leq C_{i,j-1}$, which means that two elements in the shorter distance are more likely to be clustered for carrying Self-ATT. In this way, local contexts are encouraged to be captured, as is shown in Figure 2(a).

Stacking Revised Self-ATT. To learn global contexts, we can stack these revised Self-ATT layers. When stacking, we hope that the higher layers will carry Self-ATT in bigger windows than the lower layers to capture the global contexts [45, 50]. To achieve this, for the m -th layer, we recalculate $C^{(m)}$ as $\tilde{C}^{(m)}$:

$$\tilde{C}^{(m)} = (1 - C^{(m)})\tilde{C}^{(m-1)} + C^{(m)}. \quad (6)$$

Then $\tilde{C}^{(m)}$ is used in Eq. (2) when $m > 1$ and $\tilde{C}^{(1)} = C^{(1)}$. Since $0 \leq C_{i,j}^{(m)} \leq 1$, $\tilde{C}_{i,j}^{(m)}$ is a convex combination of $\tilde{C}_{i,j}^{(m-1)}$ and 1, which means that $\tilde{C}_{i,j}^{(m-1)} \leq \tilde{C}_{i,j}^{(m)} \leq 1$.

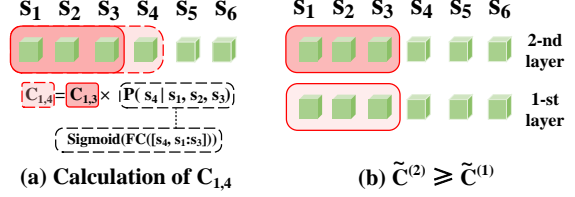


Figure 2. (a) shows how to calculate $C_{1,4}$, where the shade denotes the probability value, the darker the color, the larger the probability value. (b) shows that the clustered elements in the lower layer will be further clustered in a higher layer, *e.g.*, the color of $\{s_1, s_2, s_3\}$ in the 2-nd layer is darker than the 1-st layer.

If $\tilde{C}_{i,j}^{(m-1)}$ is large, *i.e.*, the sub-sequence $\{s_i, \dots, s_j\}$ should be clustered in the $(m-1)$ -th layer, then $\tilde{C}_{i,j}^{(m)}$ must be larger, *i.e.*, $\{s_i, \dots, s_j\}$ is also clustered in the m -th layer. For example, Figure 2(b) shows that the 2-nd layer will further cluster $\{s_1, s_2, s_3\}$ since $\tilde{C}_{1,3}^{(1)} \leq \tilde{C}_{1,3}^{(2)}$. Thus, the higher layers will carry Self-ATT in a bigger window than the lower layers to learn more global contexts.

2-D Clustering Matrix. Eq. (3) shows how to calculate C when the input is a 1-D language sequence, next we extend it to the 2-D vision surface. Given a 2-D feature map $V = \{v_{1,1}, \dots, v_{H,W}\}$, we use $C_{i,j;x,y}$ to denote the probability that softly decides whether a sub-region $\{v_{i,x}, \dots, v_{j,y}\}$ should be clustered or not, which is:

$$\begin{aligned} C_{i,j;x,y} &= P(v_{i,x}, \dots, v_{j,y}) \\ &= \prod_{k=i}^j \prod_{u=x}^y P(v_{k,u} | v_{i,x}, v_{i+1,x}, \dots, v_{k-1,u-1}) \end{aligned} \quad (7)$$

where i, j and x, y respectively denote the horizontal and vertical dimensions. To cover all the sub-regions in a $H \times W$ map, it requires applying $O(H^2 \times W^2)$ times for Eq. (4) to get all the probabilities. To reduce the computation burden, we apply the independence assumption to decompose the 2-D distribution into two independent ones, which respectively correspond to the horizontal and vertical dimensions:

$$\begin{aligned} P(v_{i,x}, \dots, v_{j,y}) &= P_h(v_{i,x}, \dots, v_{j,x}) P_v(v_{i,x}, \dots, v_{i,y}) \\ &= \prod_{k=i}^j P_h(v_{k,x} | v_{i,x}, \dots, v_{k-1,x}) \prod_{u=x}^y P_v(v_{i,u} | v_{i,x}, \dots, v_{i,u-1}), \end{aligned} \quad (8)$$

In this way, we only need to apply $O(H^2 + W^2)$ times for Eq. (4) and once matrix production. Noteworthy, as sketched in Figure 2, for the 2-D region which spans the horizontal axis from i to j and the vertical axis from x to y , we use the left-most vertical and top-most horizontal to calculate two 1-D distributions and then multiply them to get $C_{i,j;x,y}$. As Figure 3(a) shows, to calculate $C_{1,4;1,3}$, for the vertical distribution P_v , the horizontal ordinate is fixed to 1 and the vertical ordinate changes. $P_h(v_{k;1} | v_{1;1}, \dots, v_{k-1;1})|_{k=1,2,3,4}$ and $P_v(v_{1;u} | v_{1;1}, \dots, v_{1;u-1})|_{u=1,2,3}$ are calculated in the same

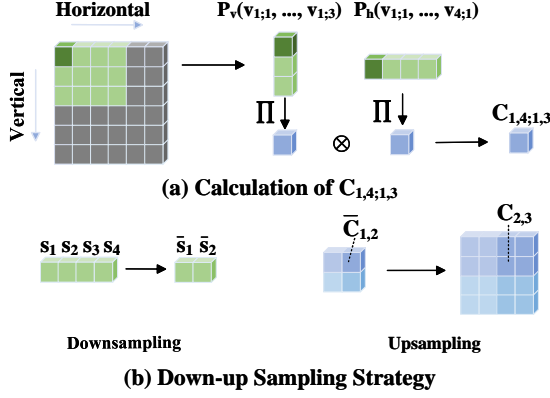


Figure 3. (a) The example of 2-D C , where $C_{1,4;1,3}$ is used as the example, which is decomposed into vertical and horizontal directions probabilities. (b) Overview of the Down-Up Sampling Strategy.

way as Eq. (4). The aforementioned symmetric characteristic is also applied.

Down-Up Sampling Strategy. If the sequence (feature map) is too long (big), we can apply the Down-Up Sampling Strategy to reduce the computation cost. We use a 1-D language case as an example to show this strategy. For $S = \{s_1, \dots, s_L\}$, we can downsample it to $\bar{S} = \{\bar{s}_1, \dots, \bar{s}_{L/2}\}$ where \bar{s}_i is the mean pooling of s_{2*i-1} and s_{2*i} . Then \bar{S} is used in Eq. (3) and Eq. (4) to get \bar{C} . To upsample \bar{C} to the original size, we set $C_{i,j} = \bar{C}_{\lceil i/2 \rceil, \lceil j/2 \rceil}$. Figure 3(b) shows one simple case where $L = 4$.

Expansion on ROI feature. The method above applies to the grid-based feature, whose feature map is formed as $H \times W$. For the ROI-based feature, the position of the regions is not certain and the regions are not arranged as grids. Given the n regions: $\{(u_1, v_1), (u_2, v_2), \dots, (u_n, v_n)\}$, where u, v represents the center coordinates, it is divided into W groups based on u . If n cannot be divided by W , we fill the last group with dummy regions until it has H regions, so that each group contains H regions. Then we sort the regions by v in each group. Finally, we obtain a sorted ROI feature map that has the same form as grid features.

3.2. Encoder-Decoder Architecture

As is shown in Figure 4, we apply the ACF to build the vision encoder and language decoder. Compared to the classic Transformer, our ACF introduces clustering-restrained attention head. Specifically, in the encoder, we calculate a 2-D clustering matrix C (cf. Eq. (7)) to softly cluster the elements for carrying Self-ATT. Similarly, in the decoder, the attention head is revised with the 1-D C (cf. Eq. (5)). The output of this encoder-decoder is used to calculate the word distributions Z .

To train our IC model, we optimize the model by minimizing the cross-entropy loss and maximizing the Reinforcement learning (RL) [38] reward. First, we train the

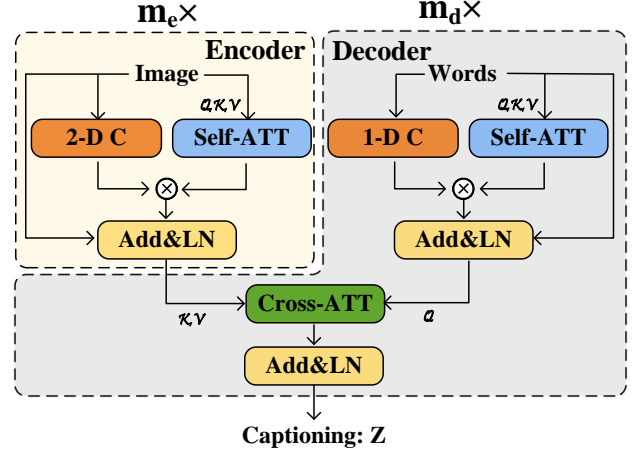


Figure 4. Overview of our ACF-based encoder-decoder IC model. The “Add&LN” is the Add and Layer Normalization. m_e/m_d represent the number of the encoder/decoder layers, respectively.

model by minimizing the cross-entropy loss:

$$L_{CE} = -\log P(Z^*), \quad (9)$$

where Z^* is the ground-truth captions. Then, we further train the model by minimizing the negative reward:

$$L_{rl} = -\mathbb{E}_{Z^s \sim P(Z)}(\mathbb{S}(Z^*, Z^s)), \quad (10)$$

where Z^s is sampled from Z , \mathbb{E} represents the mathematical expectation, and \mathbb{S} represents the evaluation metrics, e.g., CIDEr [42].

4. Experiments

4.1. Dataset, Metrics, and Settings

MSCOCO. Following [33, 50, 16, 14, 9], we train and evaluate our model on MSCOCO [23], which contains 123,287 images, and each one is annotated with 5 captions. In the experiments, we use the Karpathy split (113,287/5,000/5,000 train/val/test images) [17] for offline training and the official split (40775 test images) for online testing [2].

Metrics. We adopt five widely-used metrics in captioning for evaluation, including BLEU [34], METOR [1], ROUGE-L [39], CIDEr [42], and SPICE [3]. Besides, we calculate the fine grained alignment score [29, 54, 53] to evaluate the correspondence of the visual and language patches. Given the visual feature D_v and the text feature D_t , we firstly calculate $V_{score} = D_v \cdot D_t^T$, and $T_{score} = D_t \cdot D_v^T$, where “ \cdot ” represents the matrix multiplication. Then we count the number of coincidence of the maximum index of V_{score} and T_{score} . Finally, we normalize this number and obtain the normalized fine grained alignment score.

Settings. In the training process, we convert all the captions into lowercase and delete all the words that occur less than

6 times. The remaining 9487 words are regarded as our vocabulary. Besides training on the grid features, we also try to expand on the ROI features. In detail, we arrange the ROI as a matrix according to the position of ROI. We adopt Swin Transformer [25] as the visual encoder to extract the grid features, and Oscar [22] to extract the ROI features. The size of the grid feature map is $H \times W = 12 \times 12$, and we apply the Down-Up Sampling Strategy (cf. Section 3.1) with sampling rate 2. For the ROI feature, we set $H = 6$ without the sampling strategy. We train 20/30 epochs in the cross-entropy/RL stage. In the cross-entropy stage, the Adam optimizer is used with the learning rate of $5 \times 10^{-5}/1 \times 10^{-4}$ and decays by 0.8 per 5 epochs for grid/ROI features. In the RL stage, the learning rate is initialized to $5 \times 10^{-6}/2 \times 10^{-5}$ and we implement the same decay policy for 10 epochs for grid/ROI features. Then the “Reduce-On-Plateau” strategy is applied with a decay rate of 0.5 and patience of 3. The batch size is 40 at the whole training stage.

4.2. Ablation Studies

We conduct extensive ablations for validating the effectiveness of Ada-ClustFormer (ACF) as follows: **BASE**: we set both the encoder and decoder as the classic Transformer. **ACF_{DE}**: the decoder is set to the 1-D ACF (cf. Eq. (5)). **ACF_{EN-2D}**: the encoder is set to 2-D ACF (cf. Eq. (8)). **ACF_{EN-1D}**: the encoder is set to 1-D ACF where the vision tokens are treated as one sequence where the image patches are arranged from top-left to the bottom-right. **w/o Eq.(6)**: we remove Eq. (6) in ACF. **SR@4**: we adjust the Down-Up Sampling rate to 4 (cf. Section 3.1). **FS@2**: we use the fixed-size window in ACF where the window size is set to 2.

Table 1 shows the performance of the ablation models. Firstly, we observe that our ACF achieves the highest score, which proves its effectiveness. Next, we evaluate the effect of each module respectively. We compare ACF with ACF_{DE}, ACF_{EN-2D}, ACF_{EN-1D}, it shows that ACF achieves better results than the classic self-attention. And there is a significant improvement when the encoder and decoder are both ACF, which indicates that the unified structure can transfer more structural commonalities. Besides, the results in ACF_{EN-1D} that treating the 2-D vision tokens as a 1-D sequence can not achieve a good result. This result proves the necessity of 2-D ACF calculation instead of treating vision and language as equal modalities. By comparing with ACF and w/o-Eq.(6), it indicates that the convex constraint is necessary in ACF. It is also in line with the intuition that the higher layers carry more global semantics. The results of SR@4 imply that the Down-Up sampling strategy is a trade-off of performance and computational burden and a smaller sampling size improves the performance. Compared FS@2 with ACF, we observe that

Table 1. Performance of the ablation models.

Models	B@4	M	R	C	S
BASE	40.0	29.7	59.6	134.4	23.4
ACF_{DE}	40.2	29.8	59.9	135.1	23.7
ACF_{EN-2D}	40.4	29.8	60.0	135.9	23.7
ACF_{EN-1D}	40.0	29.4	59.4	134.5	23.2
w/o-Eq.(6)	39.1	28.7	58.8	132.6	22.8
SR@4	39.8	29.0	59.3	135.5	23.0
FS@2	39.8	29.2	59.1	134.9	22.9
ACF	41.1	30.1	60.2	137.8	24.1

ACF achieves better performance which validates the effectiveness of adaptively choosing the attention window. From another perspective, the fixed-size window is a special case of ACF, where the cluster matrix of the adjacent pair is set to 1.

Qualitative Results. We visualize the hierarchical structures of the image and the generated captions in Figure 5 according to the 2-D and 1-D clustering matrix calculated from the 1-st, 3-rd, 5-th, and 6-th layers in the encoder and decoder. By inspecting the images and captions, we can find that the patches and the words are respectively clustered, *e.g.*, in the left part of (a), the words “sitting on motorcycles” are clustered into a phrase, and in the right part, the patches in the “motorcycles” region are clustered. For ROI features, the words “a statue of a horse” are clustered in the right part of (d), and the two regions of the horse statue are clustered. More importantly, when uniting the image and caption, we can find that structural commonalities are transferred, *e.g.*, in (b), the “motorcycle” region helps generate the phrase “sitting on motorcycles”. Furthermore, the normalized fine grained alignment scores are listed in Figure 5 to evaluate the image-text alignment. We observe that ACF can improve the alignment performance in both grid-based features and ROI-based features. It implies that more structural commonalities can be transferred, benefiting from the unified clustering architecture in ACF.

4.3. Comparisons with SOTA

Comparing Methods. Nowadays, the SOTA of image captioning has been updated quickly and these models can be categorized into 3 groups. The first one is the methods that use ROI-based features, including **Up-Down** [4], **ORT** [14], **AoANet** [16], **M² Transformer** [9], **Tree-Transformer** [45], **APN** [50], and **X-Transformer** [33]. Among the above methods, Up-Down [4] deploys a famous architecture with a CNN-based encoder and an LSTM-based decoder. ORT [14] applies Transformer to language decoder. AoANet [16] and M² Transformer [9] further improve the attention mechanism on the language decoder. Tree-Transformer [45] and APN [50] reveal the validity of the utilization of the sequence structure. To capture high-order interaction between sequence and regions, X-Transformer [33] introduces a bilinear pooling struc-

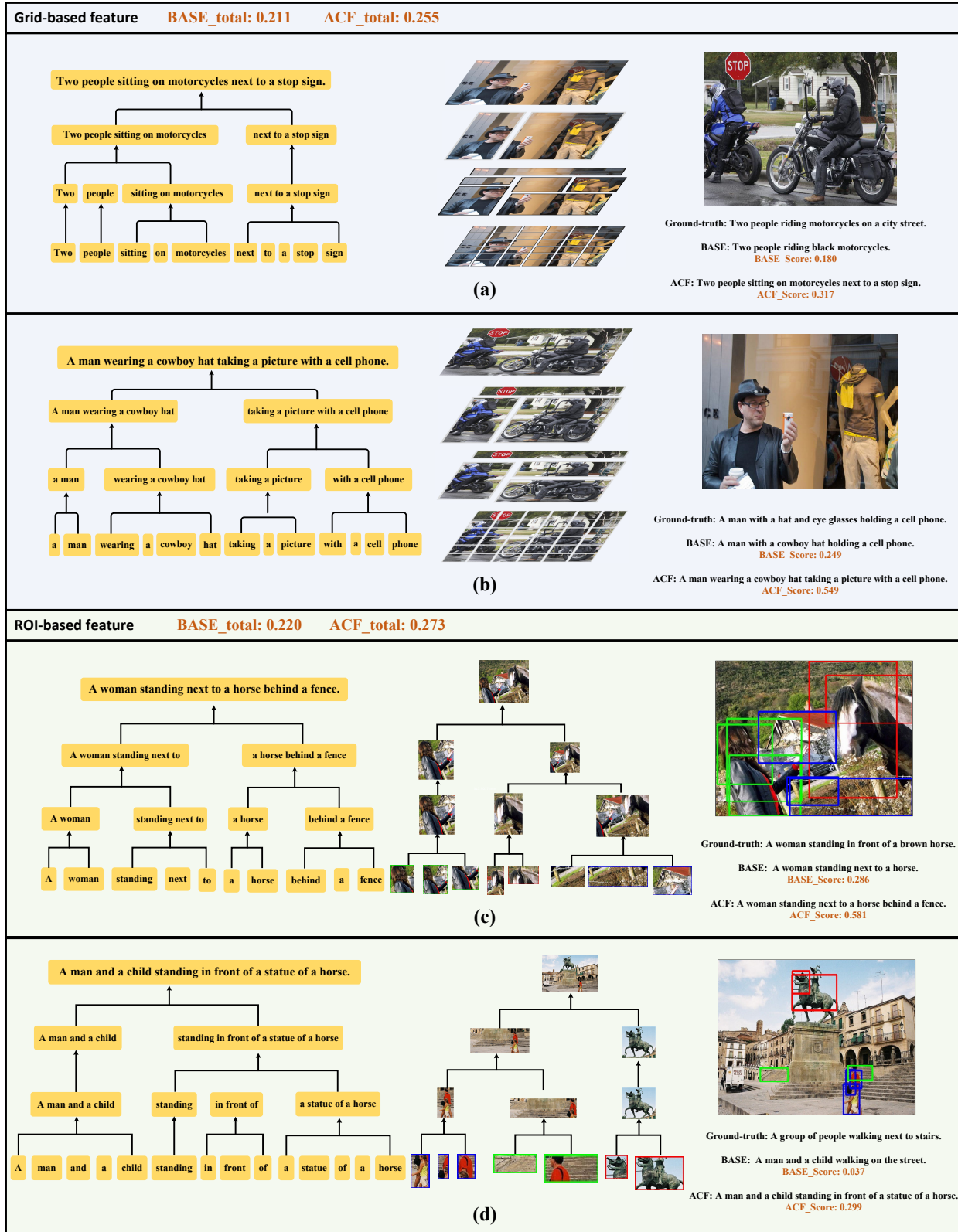


Figure 5. Examples of the generated captions by BASE and ACF model with the grid-based feature. We visualize the 2-D C and 1-D C in the 1-st, 3-rd, 5-th, and 6-th layers as the clustered patches. And the “BASE_total” and “ACF_total” represent the normalized fine grained alignment score evaluated on the whole dataset by the BASE and ACF model, respectively.

Table 2. The performances of SOTA methods on MSCOCO Karpathy split.

Models	Cross-Entropy Loss					CIDEr optimization				
	B@4	M	R	C	S	B@4	M	R	C	S
ROI-based feature										
Up-Down [4]	36.2	27.0	56.4	113.5	20.3	36.3	27.7	56.9	120.1	21.4
ORT [14]	35.5	28.0	56.6	115.4	21.2	38.6	28.7	58.4	128.3	22.6
AoANet [16]	37.2	28.4	57.5	119.8	21.4	38.9	29.2	58.8	129.8	22.4
\mathcal{M}^2 Transformer [9]	-	-	-	-	-	39.1	29.2	58.6	131.2	22.6
CATT [52]	37.3	28.5	57.4	119.0	21.5	39.4	29.3	58.9	131.7	22.8
APN [50]	-	-	-	-	-	39.6	29.2	59.1	131.8	23.0
X-Transformer [33]	38.2	28.8	58.0	122.0	21.9	39.7	29.5	59.2	132.8	23.2
Oscar-B [22]	36.5	30.3	-	123.7	23.9	40.5	29.7	-	137.6	22.8
Grid-based feature										
CPTR [24]	-	-	-	-	-	40.0	29.1	59.4	129.4	-
APN [#] [50]	-	-	-	-	-	40.1	29.4	59.4	133.2	23.3
Dual-Global [47]	-	-	-	-	-	40.3	29.2	59.4	132.4	23.3
DLCT [27]	-	-	-	-	-	40.8	29.9	59.8	137.5	23.3
PureT-base [44]	-	-	-	-	-	40.3	29.9	59.9	137.5	23.8
Visual-language BERT pretraining										
RSTNet [57]	-	-	-	-	-	40.1	28.9	59.5	135.6	23.3
ViTCAP-small [12]	35.7	28.8	57.6	121.8	22.1	40.1	29.4	59.4	133.1	23.0
ViTCAP-large [12]	36.3	29.3	58.1	125.2	22.6	41.2	30.1	60.1	138.1	24.1
VinVL [55]	-	-	-	-	-	40.9	30.9	-	140.6	25.1
ACF-ROI	36.3	28.1	57.7	123.2	21.9	40.3	29.9	60.0	138.3	23.4
ACF-Grid	38.1	28.8	58.4	123.8	21.8	41.1	30.1	60.2	137.8	24.1

Table 3. The scores on the MSCOCO online test server.

Models	B@4		M		R		C	
	c5	c40	c5	c40	c5	c40	c5	c40
Up-Down [4]	36.9	68.5	27.6	36.7	57.1	72.4	117.9	120.5
SGAE [51]	37.8	68.7	28.1	37.0	58.2	73.1	122.7	125.5
ETA [21]	38.9	70.2	28.6	38.0	58.6	73.9	122.1	124.4
APN [50]	38.9	70.2	28.8	38.0	58.7	73.7	126.3	127.6
NG-SAN [13]	38.8	70.2	29.0	38.4	58.7	74.0	126.3	128.6
Dual-Global [47]	39.1	71.2	28.9	38.4	58.9	74.4	126.3	129.2
AoANet [16]	39.4	71.2	29.1	38.5	58.9	74.5	126.9	129.6
\mathcal{M}^2 Transformer [9]	39.7	72.8	29.4	39.0	59.2	74.8	129.3	132.1
RSTNet [57]	39.7	72.5	29.3	38.7	59.2	74.2	130.1	132.4
ACF-ROI	39.3	70.7	29.4	38.7	59.1	74.2	131.0	133.1
ACF-Grid	39.0	71.3	29.2	39.2	59.2	74.2	130.2	132.3

ture. The second group are the methods using grid-based features: **CPTR** [24], **Dual-Global** [47], **DLCT** [27], and **PureT** [44]. Among them, Dual-Global [47] and DLCT [27] combine the grid-based features with the ROI-based features. PureT [44] end-to-end trains the whole model with Swin Transformer [25] as the vision encoder to deal with the visual features, which is also extracted from a Swin Transformer. Note that the PureT-base in the table is trained on two-stage. The third group distills the knowledge from large-scale pretraining models: **RSTNet** [57], **ViTCAP** [12], and **VinVL** [55]. Accordingly, we segment the performances into 3 parts in Table 2, where the top/middle/bottom parts are the ROI-based, grid-based, and BERT-based models. Note that for APN, besides reporting the results in their paper [50], which is got by using ROI-based features, we also report the performances using the same visual features as ours, which is denoted as “APN[#]”.

Results. From Table 2, we can see that ACF is comparable to most state-of-the-art performance when compared

with ROI-based and grid-based models. Moreover, ACF-Grid and ACF-ROI achieve comparable performances with ViTCAP-large [12] that distills knowledge from Google-CC [40], SBU Caption dataset [32], MSCOCO [23], and Visual Genome dataset [18], which uses 9.9M image-text pairs and 4.1M independent images to pretrain a detector-free IC model. However, we only use the captions from MSCOCO to train our ACF. Moreover, compared with APN[#] [50] which inserts an additional clustering matrix into the Self-ATT layers into the decoder, ACF achieves higher performance since it inserts the clustering matrix in both vision encoder and language decoder to build a homogeneous model.

Also, we submit the single-model results to the online server [35] for testing, which is shown in Table 3. We can see that ACF achieves the best performance than the other models, even we do not ensemble the results as AoANet [16] and \mathcal{M}^2 Transformer [9]. And we outperform the large-scale model RSTNet [57] in most of the metrics, especially in CIDEr.

5. Conclusion

We propose a novel global-local Transformer named as Ada-ClustFormer (ACF) that can adaptively cluster the input elements for carrying self-attention (Self-ATT) to learn global-local contexts. Specifically, this is achieved by inserting a clustering matrix into the Self-ATT layer, where the probability terms are calculated from the input data and thus ACF can adaptively cluster the elements. Moreover,

we use ACF to build an image captioning model to transfer more structural commonalities for better captions. The experiment results confirm the effectiveness of the proposed model.

References

- [1] Abhaya Agarwal and Alon Lavie. Meteor: An automatic metric for mt evaluation with high levels of correlation with human judgments. *Proceedings of WMT-08*, 2007.
- [2] Rami Al-Rfou, Dokook Choe, Noah Constant, Mandy Guo, and Llion Jones. Character-level language modeling with deeper self-attention. In *Proceedings of the AAAI conference on artificial intelligence*, pages 3159–3166, 2019.
- [3] Peter Anderson, Basura Fernando, Mark Johnson, and Stephen Gould. Spice: Semantic propositional image caption evaluation. In *European conference on computer vision*, pages 382–398. Springer, 2016.
- [4] Peter Anderson, Xiaodong He, Chris Buehler, Damien Teney, Mark Johnson, Stephen Gould, and Lei Zhang. Bottom-up and top-down attention for image captioning and visual question answering. In *Proceedings of the IEEE conference on computer vision and pattern recognition*, pages 6077–6086, 2018.
- [5] Peter W Battaglia, Jessica B Hamrick, Victor Bapst, Alvaro Sanchez-Gonzalez, Vinicius Zambaldi, Mateusz Malinowski, Andrea Tacchetti, David Raposo, Adam Santoro, Ryan Faulkner, et al. Relational inductive biases, deep learning, and graph networks. *arXiv preprint arXiv:1806.01261*, 2018.
- [6] Iz Beltagy, Matthew E Peters, and Arman Cohan. Longformer: The long-document transformer. *arXiv preprint arXiv:2004.05150*, 2020.
- [7] Boyu Chen, Peixia Li, Chuming Li, Baopu Li, Lei Bai, Chen Lin, Ming Sun, Junjie Yan, and Wanli Ouyang. Glit: Neural architecture search for global and local image transformer. In *Proceedings of the IEEE/CVF International Conference on Computer Vision*, pages 12–21, 2021.
- [8] Long Chen, Hanwang Zhang, Jun Xiao, Liqiang Nie, Jian Shao, Wei Liu, and Tat-Seng Chua. Sca-cnn: Spatial and channel-wise attention in convolutional networks for image captioning. In *Proceedings of the IEEE conference on computer vision and pattern recognition*, pages 5659–5667, 2017.
- [9] Marcella Cornia, Matteo Stefanini, Lorenzo Baraldi, and Rita Cucchiara. Meshed-memory transformer for image captioning. In *Proceedings of the IEEE/CVF Conference on Computer Vision and Pattern Recognition*, pages 10578–10587, 2020.
- [10] Zihang Dai, Zhilin Yang, Yiming Yang, Jaime Carbonell, Quoc V Le, and Ruslan Salakhutdinov. Transformer-xl: Attentive language models beyond a fixed-length context. *arXiv preprint arXiv:1901.02860*, 2019.
- [11] Alexey Dosovitskiy, Lucas Beyer, Alexander Kolesnikov, Dirk Weissenborn, Xiaohua Zhai, Thomas Unterthiner, Mostafa Dehghani, Matthias Minderer, Georg Heigold, Sylvain Gelly, Jakob Uszkoreit, and Neil Houlsby. An image is worth 16x16 words: Transformers for image recognition at scale. *ICLR*, 2021.
- [12] Zhiyuan Fang, Jianfeng Wang, Xiaowei Hu, Lin Liang, Zhe Gan, Lijuan Wang, Yezhou Yang, and Zicheng Liu. Injecting semantic concepts into end-to-end image captioning. In *Proceedings of the IEEE/CVF Conference on Computer Vision and Pattern Recognition*, pages 18009–18019, 2022.
- [13] Longteng Guo, Jing Liu, Xinxin Zhu, Peng Yao, Shichen Lu, and Hanqing Lu. Normalized and geometry-aware self-attention network for image captioning. In *Proceedings of the IEEE/CVF Conference on Computer Vision and Pattern Recognition*, pages 10327–10336, 2020.
- [14] Simao Herdade, Armin Kappeler, Kofi Boakye, and Joao Soares. Image captioning: Transforming objects into words. In *Advances in Neural Information Processing Systems*, pages 11137–11147, 2019.
- [15] Xiaowei Hu, Zhe Gan, Jianfeng Wang, Zhengyuan Yang, Zicheng Liu, Yumao Lu, and Lijuan Wang. Scaling up vision-language pre-training for image captioning. In *Proceedings of the IEEE/CVF Conference on Computer Vision and Pattern Recognition*, pages 17980–17989, 2022.
- [16] Lun Huang, Wenmin Wang, Jie Chen, and Xiao-Yong Wei. Attention on attention for image captioning. In *Proceedings of the IEEE International Conference on Computer Vision*, pages 4634–4643, 2019.
- [17] Andrej Karpathy and Li Fei-Fei. Deep visual-semantic alignments for generating image descriptions. In *Proceedings of the IEEE conference on computer vision and pattern recognition*, pages 3128–3137, 2015.
- [18] Ranjay Krishna, Yuke Zhu, Oliver Groth, Justin Johnson, Kenji Hata, Joshua Kravitz, Stephanie Chen, Yannis Kalantidis, Li-Jia Li, David A Shamma, et al. Visual genome: Connecting language and vision using crowdsourced dense image annotations. *International Journal of Computer Vision*, 123(1):32–73, 2017.
- [19] Hwanhee Lee, Seunghyun Yoon, Franck Dernoncourt, Doo Soon Kim, Trung Bui, and Kyomin Jung. Vilbertscore: Evaluating image caption using vision-and-language bert. In *Proceedings of the First Workshop on Evaluation and Comparison of NLP Systems*, pages 34–39, 2020.
- [20] Chenliang Li, Haiyang Xu, Junfeng Tian, Wei Wang, Ming Yan, Bin Bi, Jiabo Ye, Hehong Chen, Guohai Xu, Zheng Cao, et al. mplug: Effective and efficient vision-language learning by cross-modal skip-connections. *arXiv preprint arXiv:2205.12005*, 2022.
- [21] Guang Li, Linchao Zhu, Ping Liu, and Yi Yang. Entangled transformer for image captioning. In *Proceedings of the IEEE/CVF International Conference on Computer Vision (ICCV)*, October 2019.
- [22] Xiujun Li, Xi Yin, Chunyuan Li, Pengchuan Zhang, Xiaowei Hu, Lei Zhang, Lijuan Wang, Houdong Hu, Li Dong, Furu Wei, et al. Oscar: Object-semantics aligned pre-training for vision-language tasks. In *European Conference on Computer Vision*, pages 121–137. Springer, 2020.
- [23] Tsung-Yi Lin, Michael Maire, Serge Belongie, James Hays, Pietro Perona, Deva Ramanan, Piotr Dollár, and C Lawrence Zitnick. Microsoft coco: Common objects in context. In

- European conference on computer vision*, pages 740–755. Springer, 2014.
- [24] Wei Liu, Sihan Chen, Longteng Guo, Xinxin Zhu, and Jing Liu. Cptr: Full transformer network for image captioning. *arXiv preprint arXiv:2101.10804*, 2021.
 - [25] Ze Liu, Yutong Lin, Yue Cao, Han Hu, Yixuan Wei, Zheng Zhang, Stephen Lin, and Baining Guo. Swin transformer: Hierarchical vision transformer using shifted windows. In *Proceedings of the IEEE/CVF International Conference on Computer Vision*, pages 10012–10022, 2021.
 - [26] Jiasen Lu, Caiming Xiong, Devi Parikh, and Richard Socher. Knowing when to look: Adaptive attention via a visual sentinel for image captioning. In *CVPR*, volume 6, page 2, 2017.
 - [27] Yunpeng Luo, Jiayi Ji, Xiaoshuai Sun, Liujuan Cao, Yongjian Wu, Feiyue Huang, Chia-Wen Lin, and Rongrong Ji. Dual-level collaborative transformer for image captioning. In *Proceedings of the AAAI Conference on Artificial Intelligence*, volume 35, pages 2286–2293, 2021.
 - [28] Minh-Thang Luong, Hieu Pham, and Christopher D Manning. Effective approaches to attention-based neural machine translation. *arXiv preprint arXiv:1508.04025*, 2015.
 - [29] Yangjun Mao, Long Chen, Zhihong Jiang, Dong Zhang, Zhimeng Zhang, Jian Shao, and Jun Xiao. Rethinking the reference-based distinctive image captioning. In *Proceedings of the 30th ACM International Conference on Multimedia*, pages 4374–4384, 2022.
 - [30] Ron Mokady, Amir Hertz, and Amit H Bermano. Clip-cap: Clip prefix for image captioning. *arXiv preprint arXiv:2111.09734*, 2021.
 - [31] Van-Quang Nguyen, Masanori Suganuma, and Takayuki Okatani. Grit: Faster and better image captioning transformer using dual visual features. *arXiv preprint arXiv:2207.09666*, 2022.
 - [32] Vicente Ordonez, Girish Kulkarni, and Tamara Berg. Im2text: Describing images using 1 million captioned photographs. *Advances in neural information processing systems*, 24, 2011.
 - [33] Yingwei Pan, Ting Yao, Yehao Li, and Tao Mei. X-linear attention networks for image captioning. In *CVPR*, pages 10971–10980, 2020.
 - [34] Kishore Papineni, Salim Roukos, Todd Ward, and Wei-Jing Zhu. Bleu: a method for automatic evaluation of machine translation. In *Proceedings of the 40th annual meeting of the Association for Computational Linguistics*, pages 311–318, 2002.
 - [35] Adrien Pavao, Isabelle Guyon, Anne-Catherine Letournel, Xavier Baró, Hugo Escalante, Sergio Escalera, Tyler Thomas, and Zhen Xu. CodaLab competitions: An open source platform to organize scientific challenges. *Technical report*, 2022.
 - [36] Han Qi, Fan Zejia, Dai Qi, Sun Lei, Cheng Ming-Ming, Liu Jiaying, and Wang Jingdong. On the connection between local attention and dynamic depth-wise convolution. In *The Tenth International Conference on Learning Representations, ICLR2022, Virtual Event, April 25-29, 2022*, 2022.
 - [37] S Ren, K He, R Girshick, and J Sun. Towards real-time object detection with region proposal networks. *Advances in neural information processing systems*, 2015.
 - [38] Steven J Rennie, Etienne Marcheret, Youssef Mroueh, Jerret Ross, and Vaibhava Goel. Self-critical sequence training for image captioning. In *Proceedings of the IEEE conference on computer vision and pattern recognition*, pages 7008–7024, 2017.
 - [39] Lin CY ROUGE. A package for automatic evaluation of summaries. In *Proceedings of Workshop on Text Summarization of ACL, Spain*, 2004.
 - [40] Piyush Sharma, Nan Ding, Sebastian Goodman, and Radu Soricut. Conceptual captions: A cleaned, hypernymed, image alt-text dataset for automatic image captioning. In *Proceedings of the 56th Annual Meeting of the Association for Computational Linguistics (Volume 1: Long Papers)*, pages 2556–2565, 2018.
 - [41] Ashish Vaswani, Noam Shazeer, Niki Parmar, Jakob Uszkoreit, Llion Jones, Aidan N Gomez, Łukasz Kaiser, and Illia Polosukhin. Attention is all you need. *Advances in neural information processing systems*, 30, 2017.
 - [42] Ramakrishna Vedantam, C Lawrence Zitnick, and Devi Parikh. Cider: Consensus-based image description evaluation. In *Proceedings of the IEEE conference on computer vision and pattern recognition*, pages 4566–4575, 2015.
 - [43] Oriol Vinyals, Alexander Toshev, Samy Bengio, and Dumitru Erhan. Show and tell: A neural image caption generator. In *Proceedings of the IEEE conference on computer vision and pattern recognition*, pages 3156–3164, 2015.
 - [44] Yiyu Wang, Jungang Xu, and Yingfei Sun. End-to-end transformer based model for image captioning. In *Proceedings of the AAAI Conference on Artificial Intelligence*, pages 2585–2594, Jun. 2022.
 - [45] Yau-Shian Wang, Hung-Yi Lee, and Yun-Nung Chen. Tree transformer: Integrating tree structures into self-attention. *arXiv preprint arXiv:1909.06639*, 2019.
 - [46] Chuhan Wu, Fangzhao Wu, Tao Qi, and Yongfeng Huang. Hi-transformer: hierarchical interactive transformer for efficient and effective long document modeling. *arXiv preprint arXiv:2106.01040*, 2021.
 - [47] Tiantao Xian, Zhixin Li, Canlong Zhang, and Huifang Ma. Dual global enhanced transformer for image captioning. *Neural Networks*, 148:129–141, 2022.
 - [48] Kelvin Xu, Jimmy Ba, Ryan Kiros, Kyunghyun Cho, Aaron Courville, Ruslan Salakhudinov, Rich Zemel, and Yoshua Bengio. Show, attend and tell: Neural image caption generation with visual attention. In *International conference on machine learning*, pages 2048–2057. PMLR, 2015.
 - [49] Jianwei Yang, Chunyuan Li, Pengchuan Zhang, Xiyang Dai, Bin Xiao, Lu Yuan, and Jianfeng Gao. Focal attention for long-range interactions in vision transformers. *Advances in Neural Information Processing Systems*, 34:30008–30022, 2021.
 - [50] Xu Yang, Chongyang Gao, Hanwang Zhang, and Jianfei Cai. Auto-parsing network for image captioning and visual question answering. In *Proceedings of the IEEE/CVF International Conference on Computer Vision*, pages 2197–2207, 2021.

- [51] Xu Yang, Kaihua Tang, Hanwang Zhang, and Jianfei Cai. Auto-encoding scene graphs for image captioning. In *Proceedings of the IEEE/CVF Conference on Computer Vision and Pattern Recognition*, pages 10685–10694, 2019.
- [52] Xu Yang, Hanwang Zhang, Guojun Qi, and Jianfei Cai. Causal attention for vision-language tasks. In *Proceedings of the IEEE/CVF Conference on Computer Vision and Pattern Recognition*, pages 9847–9857, 2021.
- [53] Lewei Yao, Runhui Huang, Lu Hou, Guansong Lu, Minzhe Niu, Hang Xu, Xiaodan Liang, Zhenguo Li, Xin Jiang, and Chunjing Xu. FILIP: Fine-grained interactive language-image pre-training. In *International Conference on Learning Representations*, 2022.
- [54] Zheng-Jun Zha, Daqing Liu, Hanwang Zhang, Yongdong Zhang, and Feng Wu. Context-aware visual policy network for fine-grained image captioning. *IEEE transactions on pattern analysis and machine intelligence*, 44(2):710–722, 2019.
- [55] Pengchuan Zhang, Xiujun Li, Xiaowei Hu, Jianwei Yang, Lei Zhang, Lijuan Wang, Yejin Choi, and Jianfeng Gao. Vinvl: Revisiting visual representations in vision-language models. In *Proceedings of the IEEE/CVF Conference on Computer Vision and Pattern Recognition*, pages 5579–5588, 2021.
- [56] Hengshuang Zhao, Jiaya Jia, and Vladlen Koltun. Exploring self-attention for image recognition. In *Proceedings of the IEEE/CVF Conference on Computer Vision and Pattern Recognition*, pages 10076–10085, 2020.
- [57] Luowei Zhou, Hamid Palangi, Lei Zhang, Houdong Hu, Jason Corso, and Jianfeng Gao. Unified vision-language pre-training for image captioning and vqa. In *Proceedings of the AAAI Conference on Artificial Intelligence*, volume 34, pages 13041–13049, 2020.